

# BEAM SHAPING WITH DIFFRACTIVE OPTICS FOR LASER MICRO-WELDING OF PLASTICS

David Grewell and Avraham Benatar  
Department of Industrial, Welding and Systems Engineering  
Derek Ditmer and Derek Hansford  
Biomedical Engineering Center, The Ohio MicroMD Laboratory  
The Ohio State University

The use of near-infrared radiation to weld plastics has been well documented over the last 10 years [1,2,3]. One of the most common modes of laser welding of plastics is through-transmission infrared welding (TTIr). TTIr is based on the idea of passing light/laser radiation with a wavelength ( $\lambda$ ) between 800 and 1100 nm through one plastic component and designing the second component to absorb the laser light, see Figure 1. This wavelength is selected so that the laser light can pass through one of the components being welded. That is to say, most unfilled polymers are relatively transparent at these wavelengths. By adding a small amount of absorbing additive (such as 0.01 to 1% carbon black) to the second component, absorption of the light is promoted at the interface. This absorption results in heating and melting of the interface and with the application of a controlled clamp force, the interface is welded.

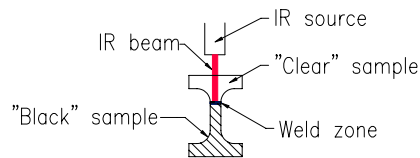


Figure 1 Basic concept of TTIr

The major breakthrough in this technology is the ability to illuminate the entire welding surface simultaneously. There are many advantages to this technology compared to heating a single spot and translating the IR spot across the welding zone, namely:

- Faster (3-10 seconds/weld)
- No problems with “run-on” / “run-off”
- Lower residual stresses
- Ability to weld to large collapses/displacements to overcome gaps at the interface

One of first concepts that allowed simultaneous illumination was based on the assembly of an array of radiation sources [4,5]. In the original designs, the spatial relationship of the array matched that of the part being welded. In later designs, light guide technology was utilized so the lasers could be remotely located for better uniformity and longer laser life [6].

A variation of this concept allowing simultaneous illumination is quasi-simultaneous welding [7]. In this mode, a single source, or a few sources, of laser(s) are steered by high speed mirrors (galvometers) to track the geometry of the part being welded. The concept relies on the ability of the system having the spot move fast enough, so that the entire surface is melted simultaneously after a number of passes.

Both the array/light guide design and quasi-simultaneous illumination have their own advantages and limitations. For example, with the light guide design, heating can be relatively uniform and fast, and scale-up is possible. However, because each tool must be designed for a particular part, it is relatively inflexible. In contrast, with high-speed scanning, it is relatively easy to reprogram the motion of the mirrors to allow different parts to be welded on the same machine. However, power limitation for a given spot (limited by equipment as well as material ablation) and shadowing effects can limit applications.

This paper reviews the feasibility of using diffractive optics to reshape a laser spot into a predefined shape so a weld can be continuously illuminated. This type of beam shaping has many of the advantages of the light guide technique, but is less complicated and should prove more efficient. For example, since there are fewer optical interfaces there should be fewer losses in the system. In addition, with diffractive optics, the beam shape is well

defined in far field ( $>$ many wavelengths) and thus can be further reshaped with standard optics. This may prove viable in making micro-welds where the image can be focused to a very small size. There are many interesting applications where small welds are needed, such as Micro-Electro-Mechanical-Systems (MEMS) [8]. One technology that is growing very fast is the use of MEMS in the medical industry. The use of thermoplastics for these applications offers significant advantages: the low manufacturing cost of polymers allows the creation of low cost, and in some cases, disposable devices. In the biomedical industry, the use of disposable devices eliminates the sterilization risks associated with reusable medical devices. This can be instrumental in cost savings, but most importantly it helps to save human lives [9]. Thus, micro-welding is a potentially large industry for the use of TTR with diffractive optics as depicted in Figure 2.

While there are many types of diffractive optic elements (DE's), the type of interest for this study is similar to those found with common laser pointers that project images for entertainment. The basic concept is the divergence of many light sources in a spherical propagation. For example, in the simplest design, two parallel slits illuminated by a collimated beam (planar wave front) such as a laser. As the light propagates from the slits, both slits act as independent light sources and the light from each propagates in a spherical shape, see Figure 3. At some distance, the two spherical waves interact with each other. In some regions, the interaction is constructive, producing "bright" regions while at  $\frac{1}{2}$  wavelengths from each of these regions are areas of destructive interference, producing "dark" regions. If a screen is placed at some distance from the slits, alternating lines of dark and bright areas are produced, see Figure 3.

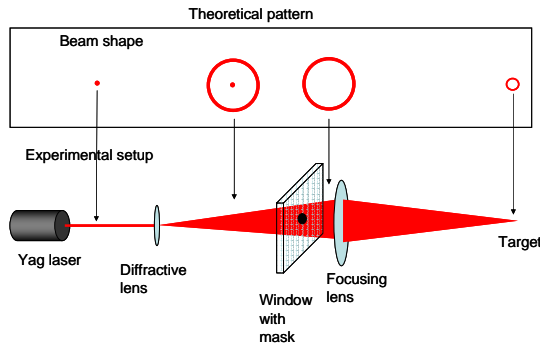


Figure 2 Diffractive optic welding system

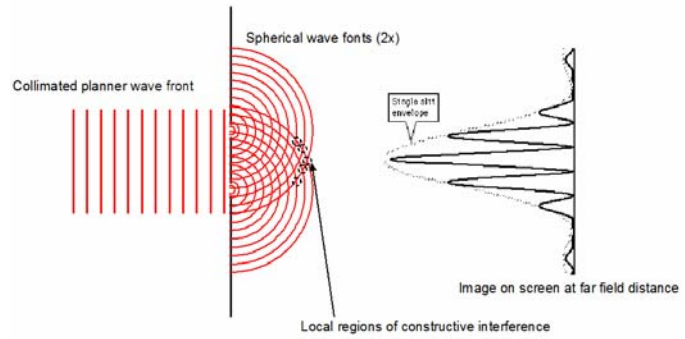


Figure 3 General concept of DE's function (Amplitude type)

In order to produce 2-dimensional patterns, such as a circle depicted in Figure 2, the line pattern is replaced by a 2-dimensional pattern, which appears very complicated. For example, Figure 4 shows a diffractive pattern which, when illuminated, produces a circle. In order to design this pattern, Inverse Fast Fourier Transforms (FFT) of complex arrays are completed [10].

In more detail, in order to design a mask to produce a circle, the image is constructed as a bitmap graphics based on the intensity mapping of the image. For example, a zero (0) is assigned to bright regions of the bitmap and a 255 level is assigned to dark regions. The image is then inverted from the center to the corners, and an inverse FFT is performed on the inverted image based on Eq 1.

$$F(K_{x,y}) = \int_{-\infty-\infty}^{\infty} \int_{-\infty-\infty}^{\infty} f(x,y) e^{-i(K_{x,y}(x)+K_{x,y}(y))} dx dy \quad [1]$$

Where  $K_x, K_y$  are the complex values of the inverse FFT. The complex values of the FFT are then truncated to 2, 4 or 8 levels, depending of the number of levels that will be fabricated in the final lens. The efficiency of the final lens is related to the number of levels. In this study, only a two-level lens was designed, so the values are truncated to either 0 or 180° phase change.

In order to determine whether the proper image will result from the predicted mask, a forward FFT can be performed on the mask array using Eq 2.

$$f(x,y) = \frac{1}{(2\pi)^2} \int_{-\infty-\infty}^{\infty} \int_{-\infty-\infty}^{\infty} F(K_{x,y}) e^{-i(K_{x,y}(x)+K_{x,y}(y))} dK_x dK_y \quad [2]$$

As seen above, the magnitude is reduced by a factor of  $(2\pi)^2$  so the magnitude has to be adjusted accordingly. Also, the image must again be inverted from corners to centers.

This type of DE design is referred to as a direct design, which results in non-optimized performance. For example, a significant amount of energy of the original beam will be passed through the zero order, which corresponds to passing straight through the center, as seen in Figure 2. As seen in the figure, this “hot-spot” can be masked out with a spatial filter. Other artifacts of a direct design include, 2<sup>nd</sup>, 3<sup>rd</sup>, etc. orders being formed, which reduce the efficiency of the lens as well as producing noise within the image that makes it fuzzy (low fidelity). In order to improve the design of a DE, alternative techniques, based on stochastic algorithms, have been developed which produce much higher efficiency DE’s compared to the DE’s designed with the direct technique. That is to say, they have lower intensity 0<sup>th</sup> and 2<sup>nd</sup>, 3<sup>rd</sup>, etc., order diffractive images and most of the energy is delivered to the desired 1<sup>st</sup> order image. It is beyond the scope of this paper to review these techniques, but it will be stated that in order to find alternative solutions, randomly generated number patterns are evaluated as the DE design. The pattern from the DE ( $F_{x,y}$  as seen in Eq 2) is then compared to the desired pattern ( $A'_{x,y}$ ) using a merit function (Eq 3). The DE is then randomly altered slightly and a new merit function is calculated in order to determine if the alteration improved the DE design. This is repeated until a desired pattern is produced [11]. This type of approach is typically computationally intensive.

$$Merit = \frac{1}{x,y} \sum_{x,y} (|F_{x,y}^1| - A'_{x,y})^2 \quad [3]$$

The last major efficiency improvement of a DE is not to block approximately 50% of the light as previously detailed but, instead to allow approximately 100% of the light to pass through the DE. This is accomplished by using the same design as previously detailed, but slowing down portions of the light instead of blocking portions of the light. That is to say, it is possible to fabricate a lens with local thickness changes equal to the approximate wavelength of light in the lens media. Thus, when the light exits the lens, the phase difference of the individual elements results in the destructive and constructive interference, see Figure 5. With this type of lens and with the proper design, it is possible to achieve greater than 70% efficiencies.

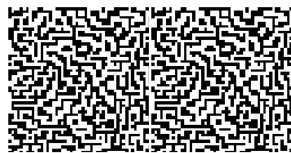


Figure 4 Diffractive pattern to produce a circle

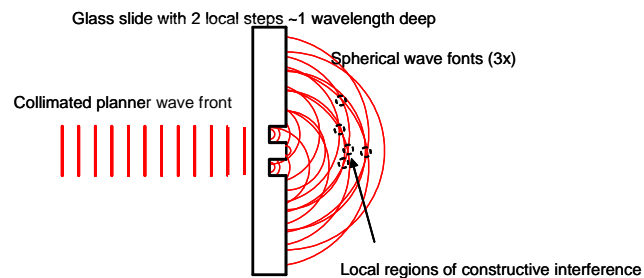


Figure 5 Example of DE with phase change

This work was undertaken as a feasibility study on the use of computer-generated DE’s for welding plastics. The DE’s were not optimized to further evaluate the importance of design optimization as well as robustness of lens fabrication. That is, this paper does answer the question “can low quality DE’s be used to weld plastics?”

## Experimentation

The DE mask image was designed using code written in Mathcad. The primary desired beam shape was a ring pattern as seen in Figure 4. Alternative shapes were also evaluated with similar results, such as a square design. It was based on a two-level lens design with a 50 x 50 pixel resolution. The images were tiled 4 times to produce a 200 x 200 pixel map, in order to assure the lens aperture was larger than the beam size. The image was then printed on a transparency with a 3800 DPI resolution. And the transparency was then mounted onto a standard mask frame for lithography.

The lens was fabricated using standard lithography techniques. The substrate was a 100 mm diameter fused silica wafer, with a thickness of 1 mm, polished on both sides. A positive photoresist (Shipley 1813) was spin-coated on the wafer to produce an approximate thickness of 1.2  $\mu\text{m}$ . The photoresist was soft-baked at 95°C for 30 minutes in

a nitrogen purged oven. The photoresist was over exposed (x2) in order to reduce speckle patterns produced by the transparency. In addition, a blank, black wafer was placed below the wafer in order to reduce back reflection of the UV radiation. This is typically not an issue, but because the fused silica wafer was transparent to the UV radiation, through transmission and back reflection is possible and it produced un-wanted patterns on the wafer. The final wafer was then etched with reactive ion etching [12], for 3.5 hours. The power was 350 W and the gasses were  $CF_4$  at  $30\text{ cm}^3/\text{min}$ . and a buffer gas of argon at  $15\text{ cm}^3/\text{min}$ .

The resulting lens was evaluated for performance in terms of uniformity of the desired beam shape, efficiency and divergence. Two lenses were designed: one with  $20\text{ }\mu\text{m}$  and another with  $30\text{ }\mu\text{m}$  features. The laser source for welding was a  $1064\text{ nm}$  wavelength YAG laser (Spectra Physics, 50W Tornado). The raw beam size was approximately  $10\text{ mm}$  in diameter. The beam was collimated to a beam diameter of  $3\text{ mm}$ . Welds were made between transparent PE film (thickness= $50\text{ }\mu\text{m}$ ) and black PE sheets (thickness= $6\text{ mm}$ ) using the experimental layout seen in Figure 2. Welds were made at various power levels and time durations.

## Results and Discussion

Before welds were made, the resulting lenses were evaluated. Figure 6 shows a photograph of the photo resist. The clear regions correspond to regions where the mask prevented UV exposure, and the photo resist was not cross-linked, leaving behind no photo resist once developed. The “hazy” region is where the photo resist was exposed. The haziness is caused by small particles and imperfections in the standard transparency that was used. Thus, the resulting lens would have imperfections. Figure 7 shows an SEM image of the resulting lens with the previously mentioned mask. It is seen that because of the haziness of the mask, there are rough areas on the lens. Thus, the lens primarily acted as amplitude design DE. Figure 8 shows a cross sectional scan from an atomic force microscope (AFM) across a single feature. It is seen that the depth of the feature is only  $420\text{ nm}$  while the desired depth is  $1220\text{ nm}$ . In addition, the AFM indicated that the side walls of the features had a profile angle of  $17^\circ$ .

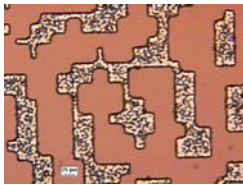


Figure 6 Picture of photo resist with  $30\text{ }\mu\text{m}$  features

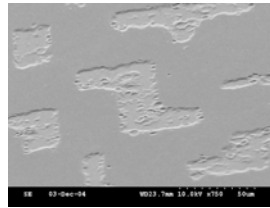


Figure 7 SEM of DE with amplitude design

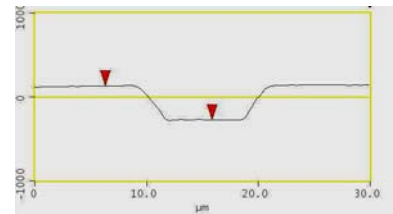


Figure 8 AFM cross sectional profile of channel

The power going into the DE's was measured at  $10.1\text{ W}$ . The transmitted beam power from the DE was  $9.27\text{ W}$ . Thus, the overall transmission of the lens was  $91.7\%$ . The power to target, after masking of the zero (hot spot), was  $0.75\text{ W}$ . Thus the overall efficiency of the lens is only  $7.4\%$ . This is not unexpected, because direct algorithms were used to design the lens and the lithography mask had impurities. Future results with better designs and masks should provide much higher efficiencies. With the  $20\text{ }\mu\text{m}$  feature size DE, the ring diameter was  $11.9\text{ mm}$  at a working distance of  $140\text{ mm}$  resulting in an image divergence of  $2.4^\circ$ . The  $30\text{ }\mu\text{m}$  feature size had an approximate image divergence of  $1.6^\circ$ .

Figure 9(a) shows a typical “burn” pattern from the DE directly, where a burn pattern is the image produced on special (zap) paper for laser spot analysis. It is seen that the geometry of the pattern is very close to the desired image; however, the uniformity of the image is relatively poor. Figure 9(b) shows a similar image, except that the image is focused (as seen in Figure 2) using a lens ( $15\text{ mm}$  focal length). It is seen that, again, the image geometry is similar to the desired image and the focusing lens allows for image size reduction; however, the uniformity is relatively poor.

Figure 10 shows welds made with various heating times with  $1.5\text{ W}$  of power at the weld interface. It is seen that it takes as long as  $20\text{ s}$  to make a weld. However, the quality appears relatively good. Lower laser power settings produced welds, but, as expected, the cycle times were relatively long and because of thermal diffusion, the weld definition was relatively poor.

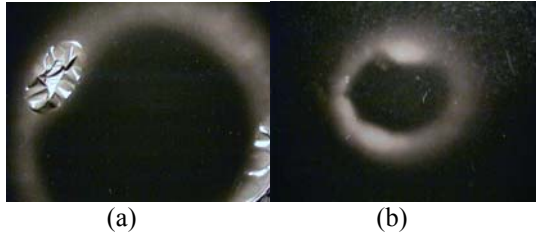


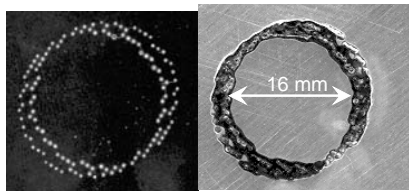
Figure 9 Typical burn pattern from DE (a:11.8 mm dia.) and with focusing lens (b: 4 mm dia.)



Figure 10 Pictures of welds at various heating times

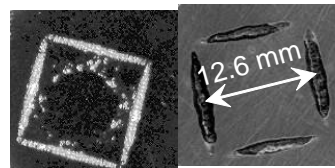
Based on the initial findings, additional lenses were fabricated where the photoresist was over exposed (x3) in order to remove haziness from the final DE. Figure 11 shows a burn pattern and weld, respectively, with the lens fabricated with an over exposure. It is seen that the fidelity of the lens is such that the pixels of the original bitmap can be easily seen. It is also seen that the original bitmap was not exactly on center and thus, the 1<sup>st</sup> and 2<sup>nd</sup> order images are slightly shifted relative to each other (two circles).

Figure 12 shows similar results with a square pattern generated with a lens fabricated with an over exposure of the photoresist. Again the fidelity is relative good; however, the corners of the square are slightly under welded. It is anticipated that this can be corrected by adjusting the local intensity of the original bitmap. The efficiency of this lens was measured to be 56%. That is to say, 56% of energy went to the desired image while the balance of the energy went to higher orders and the zero order (hot spot).



Burn image Weld on PC  
(2.0 sec @ 80 W  
fiber laser 1084 nm)

Figure 11 Circle patterns with clear DE lens



Burn image Weld on PC  
(2.0 sec @ 80 W  
fiber laser 1084 nm)

Figure 12 Square patterns with clear DE lens

## Conclusions

It is seen that it is possible to use diffractive optical elements to reshape laser beams for welding of plastics. In addition, even with relatively low efficiency designs, with a relatively low quality laser and poorly fabricated lens, welds can be produced. These same images can also be resized with standard optical elements. Thus, future improvements in DE design should make it possible to use this concept in industrial applications.

## Acknowledgements

Special thanks go to Mark Crawford of OSU, Todd Lizotte of Hitachi Via Mechanics (USA) and Prof. Donald C. O'Shea of Georgia Institute of Technology for their help.

## References

1. Yeh, H., Grimm, R., Infrared Welding of Thermoplastics, Characterization of Transmission Behavior of Eleven Thermoplastics, ANTEC-98 Conference Proceedings, Society of Plastics Engineers, Brookfield, CT
2. Potente H., Becker F., Weld Strength Behavior of Laser Butt Welds, ANTEC-99 Conference Proceedings, Society of Plastics Engineers, Brookfield, CT
3. Grewell, D., Applications with infrared welding of thermoplastics, ANTEC-99 Conference Proceedings, Society of Plastics Engineers, Brookfield, CT

4. US Patent 5,740,314; IR heating lamp array with reflectors modified by removal of segments thereof, Robert A. Grimm
5. US Patent 6,205,16, Laser Diode Array, David Grewell
6. US Patent 6,528,755, Light guide for laser welding, David Grewell, Justin Bickford, Donald Lovett, Paul Rooney
7. H. Potente, G. Fiegler, F. Becker and J. Korte, Comparative Investigations on Quasi-Simultaneous Welding on the Basis of the Materials PEEK and PC, ANTEC-02 Conference Proceedings, Society of Plastics Engineers, Brookfield, CT
8. Grewell, D. Benatar, A. Experiments in Micro-Welding of Polycarbonate with Laser Diodes, ANTEC-02 Conference Proceedings, Society of Plastics Engineers, Brookfield, CT
9. H. Becker, C. Gärtner, Polymer micofabrication methods for microfluidic analytical application, Electrophoresis 2000, Vol. 21, pp 12-26, VCH-Wiley Verlag, Weinheim
10. D., O'Shea, et al., Diffractive Optics, Design, Fabrication and Test, pp 57-83, 2004, SPEI Press, Bellingham, WA
11. W. Saxton, R., Gerchberg, A Practical Algorithm for the Determination of Phase from Image and Diffractive Plane Pictures, Optik, 35, pp 237-249, 1972
12. Madou, M. Fundamentals of Microfabrication, The Science of Miniaturization, pgs 87-97, 2002, CRC Press, Boca Raton, FL